Title
Coherent structures in electrostatic interchange mode turbulence

Permalink
https://escholarship.org/uc/item/26p0g5cf

Journal
Physica Scripta, 74(6)

ISSN
0031-8949

Author
Shaikh, D

Publication Date
2006-12-01

Peer reviewed

Coherent structures in electrostatic interchange mode turbulence

Dastgeer Shaikh[*]

Institute of Geophysics and Planetary Physics,

University of California, Riverside, CA 92521.   USA.

Abstract

Exact nonlinear coherent vortex solutions, in the form of dipolar like configuration, are derived in a two dimensional electrostatic interchange turbulence model. The vortex structure incorporates effects due to nonlinear diamagnetic interactions that are associated with finite Larmour radius of the magnetized ions. Numerical simulations indicate that propagating dipole vortex is a long-lived, spatially well localized coherent structure of the interchange mode that persists for several eddy turn-over time. Collisional as well as weak diamagnetic interactions have stabilizing effects on these structures.

---
[*] Electronic mail: dastgeer@ucr.edu

I. INTRODUCTION

Large scale nonlinearly localized coherent structures such as zonal flows, streamer and vortices in low frequency ($\omega \ll \omega_{ci}$) electrostatic turbulence are widely believed to be responsible for determining the level of ion thermal transport in the magnetically confined hot tokamak plasmas [1–6]. Considerable attention have therefore been given recently to understand dynamics of these structures based upon fluid models, such as low-frequency drift wave turbulence and its several invariants, and kinetic models owing particularly to their occurrence in several tokamak and spheromak experimental plasmas. For instance, Hamada et al [7] have shown in JIPP T-llU Tokamak Plasmas that the low-density Ohmically heated tokamak plasmas have streamer-like eddies at the outer region at minor radius. The radial span of the eddies is estimated to be much larger than the poloidal span. Oscillatory zonal flows, also called geodesic acoustic modes (GAMs) are shown to exist in a high safety factor region of tokamak plasmas [8]. The geodesic acoustic mode (GAM) zonal flows is also identified in HL-2A tokamak plasmas, where high coherence of both the GAM and the ambient turbulence for the toroidally displaced measurements along a magnetic field line is observed [9]. Similarly, JFT-2M tokamak reported the higher frequency fluctuations as geodesic acoustic modes (GAMs) zonal flows [10]. Furthermore, transport improvement due to increased shear flow arising from the zonal flow structures are observed in the DIII-D tokamak [11]. These work, only a few experimental studies that are mentioned here amongst many other, nevertheless reveal that transport properties are significantly governed by the nonlinear saturated structures. Correspondingly, there have been significant efforts gone into understanding these nonlinear structures. For example, recent gyrokinetic simulations demonstrate how turbulent transport is influenced by the nonlinear zonal and streamer structures [12], while they may evolve further to form long-lived coherent structures [6]. The two dimensional (2D) simulations of ion temperature gradient (ITG) mode also reveal an existence of the long-lived, large scale coherent structures in the presence of a magnetic shear as well as in a local coordinate system [13, 14]. These structures continue to appear even in the nonlinear evolution stage and may possibly influence the level of the anomalous transport in the magnetically confined tokamak plasmas. Nycander [15] et. al. have demonstrated the persistence of a monopolar vortex in η_i modes turbulence. Moreover, the presence of quasi coherent structures in the ITG turbulence has also been demonstrated

2

experimentally [16]. Motivated by these results, we in the present paper concentrate specifically on investigating the nonlinearly saturated coherent structures in the low frequency interchange mode turbulence [17] which is one of the variants of the drift wave turbulence with $k_\parallel \approx 0$, where $k_\parallel$ is a mode parallel to the confining magnetic field.

The flute-type electrostatic interchange mode turbulence model uses the electron continuity equation instead of the adiabatic massless electrons moving parallely along the magnetic field lines with finite $k_\parallel$ [17]. The ion temperature effects have been incorporated in the ion continuity equation through ion Finite Larmour Radius (FLR) term. This is a reasonably simple model, which can be useful to describe the tokamak edge region and under suitable conditions gives rise to the curvature driven mode, known as the Rayleigh-Taylor (RT) instability [18]. The flute-type instabilities are invariably intrinsic to the tokamak plasmas confined by a strong curved magnetic field. Moreover the set of equations describing interchange mode turbulence are essentially different from the most commonly implied plasma model such as drift waves and its other derivatives [19, 20] in terms of the nonlinear character. Unlike the latter, the nonlinear manifestations due to the simultaneous existence of convective ($\mathbf{E} \times \mathbf{B}$) and diamagnetic nonlinearities, and their inter-play in the presence of an additional polarization nonlinearity, are rather subtle and are more or less unexplored. In the present work, we therefore investigate the nonlinear properties of the interchange mode turbulence by seeking its exact nonlinear coherent solution, and understand its detailed dynamics purely in a state of isolation. Following the analytic treatment as used earlier [21, 22], we find that nonlinear interchange modes admit exact stationary solution in the form of dipole vortex in a moving frame of reference. Our investigations based upon collisional interactions between two such coherent structures indicate that they are long-lived, fairly stable structures which continue to persist for sufficiently large number of turn over time and preserve momentum conservations.

After describing basic equations, conservation properties and the linear dispersion of this model in section II, an exact nonlinear solution are obtained analytically in section III. Simulation results for a translating dipole vortex and mutual interaction between two such structures are considered in section IV and V respectively. The conclusions are discussed in section VI.

II.   BASIC EQUATIONS

The two dimensional electrostatic interchange mode turbulence for a quasi-neutral plasma has been considered under the limit of cold ion plasma immersed in a curved magnetic field. The basic equations can readily be cast in terms of two scalar variables, namely, fluctuating density and electrostatic potential [17],

$$\frac{\partial n}{\partial t} + \epsilon_n \frac{\partial n}{\partial y} + (1 - \epsilon_n)\frac{\partial \phi}{\partial y} + \hat{z} \times \nabla\phi \cdot \nabla n = D\nabla^2 n \tag{1}$$

$$\left(\frac{\partial}{\partial t} - \tau\frac{\partial}{\partial y}\right)\nabla^2\phi + \epsilon_n(1+\tau)\frac{\partial n}{\partial y} + \hat{z} \times \nabla\phi \cdot \nabla\nabla^2(\phi + \tau n) = \mu\nabla^4\phi \tag{2}$$

Equation (1) is the electron continuity equation, while Eq. (2) represents the ion vorticity equation. The diamagnetic terms are associated with the parameter $\tau = T_i/T_e$, the ratio of ion to electron temperatures, and appears in linear as well as in nonlinear terms. The other dimensionless variables and parameters, i.e., electrostatic potential, electron density, time, spatial co-ordinates are respectively $\phi = e\tilde{\phi}L_n/T_e\rho_s, n = \tilde{n}L_n/N\rho_s, t = t'L_n/C_s, (x, y) = (\bar{x}, \bar{y})/\rho_s, \epsilon_n = 2L_n/R$, where $e, L_n, \rho_s, N, C_s, R, \mu$, and D are respectively electric charge, density gradient length scale, ion Larmour radius, total density, sound speed, major radius of tokamak, viscosity, and particle diffusivity. Equations (1) & (2) can yield following conservation law,

$$\frac{1}{2}\frac{\partial}{\partial t}\int \left[n^2 + (\nabla\phi)^2\right] dxdy + (1 + \epsilon_n\tau)\int n\frac{\partial\phi}{\partial y}dxdy = -\int \left[D(\nabla n)^2 + \mu(\nabla^2\phi)^2\right] dxdy, \tag{3}$$

which shows that the rate of change of total energy (pressure + kinetic) decays due to the flux, diffusivity and viscosity effects. The linear eigen frequency of Eqs. (1) & (2) can be readily obtained by dropping the nonlinear terms and further by assuming that the perturbed quantities, i.e. (n, ϕ), depend sinusoidally on the frequency ω and wavenumber $\mathbf{k} = (k_x, k_y)$ as $\exp(-ik_x x - ik_y y - i\omega_k t)$. The perturbed density and vorticity equations then can be written in the linearized from in the (k, ω)-space as follows.

$$-i\omega_k n_k - i\epsilon_n k_y n_k - i(1 - \epsilon_n)k_y\phi_k = 0.$$

$$i(\omega_k - \tau k_y)k^2\phi_k - i\epsilon_n(1 + \tau)k_y n_k = 0.$$

Note that the diffusion (D) and viscosity (μ) terms are ignored here as they are responsible for damping of the modes only while the growth rate of the linear instability will be determined entirely by the diamagnetic and convective terms. Eliminating n_k and ϕ_k from the

4

above coupled linear equations, we obtain the following eigen frequency relation.

$$\omega_k = \frac{k_y}{2}(\epsilon_n - \tau) + i\frac{k_y}{k_\perp}\sqrt{\epsilon_n(1 - \epsilon_n)(1 + \tau)}\left\{\frac{k_\perp^2(\epsilon_n + \tau)^2}{4\epsilon_n(1 - \epsilon_n)(1 + \tau)} - 1\right\}^{1/2}.$$

It is noteworthy that for positive real frequency (i.e. $\epsilon_n > \tau$), the modes move in the direction of the electron diamagnetic drift, while in the opposite case (i.e. $\epsilon_n < \tau$) they move along the ion diamagnetic drift.

III. STATIONARY DIPOLE VORTEX SOLUTIONS

The two dimensional traveling wave solutions of Eqs. (1) & (2) in the moving frame can be obtained by supposing $x = x, y = y - ut, t = t$, where u being the speed of the vortex. This further transforms the fluctuating quantities into $n(x, y, t) = n(x, y)$ and $\phi(x, y, t) = \phi(x, y)$. The fluctuation density, and potential obey localized boundary conditions $\phi, n \rightarrow 0$ as $y \rightarrow \infty$ for all x. The condition of localization associated with the coherent structures further enables us to use the periodic boundary conditions in computational domain of the nonlinear fluid simulations, to be discussed in the subsequent section. The periodic region in our simulations further corresponds to a local physical region in the tokamak devices. The perturbed entities, or coherent structures, in the local region are far from the boundary and can translate freely. Hence no boundary effects are considered in our analysis. Boundary effects can nevertheless be important for certain processes, but this issue is well beyond the scope of present work. Moreover, the $x - y$ plane in the simulations is orthogonal to the background magnetic field in the tokamak geometry. On using the transformed co-ordinate systems, the electron continuity and the ion vorticity equations can be translated into a co-ordinate system that is moving along y-direction with the vortex speed. Following the treatment described by Larichev & Reznik [21], we in the following demonstrate how nonlinear interactions are responsible for the generation of a large scale stationary vortex. Firstly, the electron continuity yields following relation [15, 19, 22]

$$[n - (1 - \epsilon_n)x, \ \phi + (\epsilon_n - u)x] = 0,$$

Note that in a moving (with velocity u) vortex frame, the local co-ordinate transformation are chosen as $x = x, y = y - ut$. In this moving frame, the time derivative in both the density and vorticity Eqs. (1) & (2) can be replaced by the convective derivative such that

5

$\partial/\partial t = -u\partial/\partial y$. Here $[,]$ represent the nonlinear Poisson brackets with respect to the spatial derivatives x, y. The vanishing of Poisson brackets essentially means $B = F(A)$, if $[A, B] = 0$ (i.e. when $[A, B] = 0$ then B can be expressed as an arbitrary function of A such that $B = F(A)$). The function F is an arbitrary function of its argument and is continuous and differential within and outside the region of vortex boundaries. This properties allows one to write electron continuity equation in the following form,

$$\phi + (\epsilon_n - u)x = F\left(n - (1 - \epsilon_n)x\right),$$

where F could be an arbitrary function of its argument. Next using the boundary as well as the localization conditions as stated above, potential and density can be related to each other through the following relation.

$$\phi = \left(\frac{\epsilon_n - u}{\epsilon_n - 1}\right)n. \tag{4}$$

Upon substituting $\phi = F + (u - \epsilon_n)x$ in the ion vorticity equation which is being transformed into a moving co-ordinate system of the vortex having speed u, we get the following Poisson bracket,

$$\left[\nabla^2 n - \left\{\frac{\epsilon_n(1 + \tau)(\epsilon_n - 1)^2}{(\epsilon_n - u)[\epsilon_n - u + \tau(\epsilon_n - 1)]}\right\}x, \; n - \left\{\frac{(u + \tau)(\epsilon_n - 1)}{\epsilon_n - u + \tau(\epsilon_n - 1)}\right\}x\right] = 0.$$

This equation, again due to the property of Poisson brackets, can further be written down as,

$$\nabla^2 n - \frac{\epsilon_n(1 + \tau)(\epsilon_n - 1)^2}{(\epsilon_n - u)[\epsilon_n - u + \tau(\epsilon_n - 1)]}x = G\left(n - \frac{(u + \tau)(\epsilon_n - 1)}{\epsilon_n - u + \tau(\epsilon_n - 1)}x\right) \tag{5}$$

where G is also an arbitrary function of its argument. We seek localized solution of Eq. (5), as obtained by Meiss et al [22]. Thus for all x and $y \to \infty$, the density $n \to 0$, readily yields the following functional form of the function G,

$$G(\alpha) = \frac{\epsilon_n(1 + \tau)(\epsilon_n - 1)^2}{(u + \tau)(\epsilon_n - u)}\alpha$$

where α is an arbitrary function of G, when substituting it in above eqns, we get

$$\nabla^2 n = \left(\frac{\beta^2}{a^2}\right)n \tag{6}$$

where

$$\frac{\beta^2}{a^2} = \frac{\epsilon_n(1 + \tau)(\epsilon_n - 1)^2}{(\epsilon_n - u)[\epsilon_n - u + \tau(\epsilon_n - 1)]}$$

6

The Eq. (6) represents an equation of vorticity whose solution essentially gives rise to vortex like configuration. However the isolation of the vortices require that the phase speed must satisfy $\beta^2/a^2 > 0$ in Eq. (6). This further puts some stringent condition on the existence of nonlinear interchange mode structures. An analysis of this condition is depicted in Fig (1), which recognizes permissible range of characteristic wavenumbers for which vortex solution is likely to exist. The upper region in the figure takes on positive values of allowed speed. This region essentially corresponds to electron diamagnetic direction, while the lower region in Fig(1) represents ion diamagnetic region for the interchange mode turbulence vortices.

We next seek an exact stationary solution of Eq. (6) in the interior as well as exterior region of a vortex of finite radius (r). Equation (6) can have dipolar configuration solution in the exterior region which are sum of the modified Bessel function as given below.

$$n(r,\theta) = AK_1\left(\frac{\beta}{a}r\right)\cos\theta, \quad r > a \tag{7}$$

where $r^2 = x^2 + y^2$, $\cos\theta = x/r$, $\sin\theta = y/r$ and $\theta = \tan^{-1}(y/x)$. The argument of the function G leads to the contours of $\Lambda = n - \bar{\xi}x$, where $\bar{\xi} = (u+\tau)(\epsilon_n-1)/[\epsilon_n-u+\tau(\epsilon_n-1)]$, and may extends upto infinity. In principle, Eq. (6) can exhibit many classes of vortex solutions depending upon the choice of the arbitrary function F (which is linear for a class of vortex solution given above). For instance, for a quadratic form of F, Eq. (6) can admit quadrapolar like vortex configuration. We will not however discuss other form of the vortex solution here, as they are beyond the scope of the present work. Nevertheless the coherent structures must be finite within the extent of their localization. Therefore vorticity contours have to be finite within a circle of radius $r = a$ where $\Lambda = 0$. Hence the functional form of G is chosen in such a manner that the function and its derivative are continuous across $r = a$. With these arguments, functional form of G has been chosen to be linearly dependent on its argument in the interior region, as follows,

$$G(\alpha) = \left(\frac{\gamma^2}{a^2}\right)\alpha.$$

The interior solution of Eq. (5) due to linearly dependent form of G is then,

$$n(r,\theta) = \frac{Br}{a}\cos\theta + CJ_1\left(\frac{\gamma}{a}r\right), \quad r < a \tag{8}$$

It can be noticed here that Eqs. (7) & (8) have dependence on $\cos\theta$ and modified Bessel functions, which essentially lead to vortex solution that has dipolar spatial configuration

within the bounded region of the vortex radius r. The other constants are determined from the conditions of continuity and differentiability of n & ϕ, which yield

$$A = \frac{a}{K_1(\beta)} \frac{(u + \tau)(\epsilon_n - 1)}{\epsilon_n - u + \tau(\epsilon_n - 1)},$$

$$B = a \left[\frac{(u + \tau)(\epsilon_n - 1)}{\epsilon_n - u + \tau(\epsilon_n - 1)} + \frac{\beta^2}{\gamma^2} \right],$$

$$C = -\frac{\beta^2}{\gamma^2} \frac{a}{J_1(\gamma)}.$$

Here γ is determined by the roots of nonlinear dispersion relation given as follows,

$$\frac{\beta}{\gamma} \frac{J_2(\gamma)}{J_1(\gamma)} + \left[\frac{(u + \tau)(\epsilon_n - 1)}{\epsilon_n - u + \tau(\epsilon_n - 1)} \right] \frac{K_2(\beta)}{K_1(\beta)} = 0. \tag{9}$$

The nonlinear dispersion relation Eq. (9) can in principle lead to a set of infinite roots as $\gamma_n(\beta)$, with $n = 1, 2, 3, \cdots$. The roots obtained from its numerical solution are shown in Fig (2). It can be seen from the figure that for a given value of β there can exist multiple roots. Thus for a given value of β, using one of the multiple roots of γ and using other parameters for the dipole vortex such as r, u, (which are vortex radius, speed) a dipole vortex can be constructed as shown in Fig(3).

In the rest part of the paper, various dynamical features of the interchange mode dipole vortex are investigated using two dimensional numerical computations. These include translational property, collisional interactions, and stability etc.

IV. TRAVELING DIPOLE VORTEX

The propagating dipole vortex of interchange mode turbulence are studied by numerical simulation. For this purpose, the two field interchange mode Eqs. (1) & (2) are numerically integrated in an ideal limit when $\mu, D \to 0$ using a fully de-aliased pseudospectral scheme [23]. Periodic boundary conditions are employed along the x and the y-directions. The evolution variables n, ϕ are discretized in Fourier space. The linear part of Eqs. (1) & (2) is integrated exactly. The nonlinear terms are evaluated in real space and then Fourier transformed in k-space by going back and forth in real and k-space at each time step. The Fast Fourier Transform (FFT) routines are used to go back and forth in the real and k-space at each time integration. The time advancement is done using predictor corrector with the mid point leap frog scheme. The spatial resolution varies from 128^2 to 256^2 Fourier modes.

It is confirmed that change of spatial resolution or computational domain size do not alter any physical observable features of the dipolar vortex in our simulations. Most of the results presented here would correspond to spatial resolution due to 128×128 Fourier modes along the x and the y-directions. The numerical accuracy of the code is ensured continuously by monitoring the energy conservation relation [Eq. (3)] at each time step. The linear diamagnetic frequency associated with the curvature terms in the nonlinear interchange mode Eqs. (1) & (2) is held fixed with respect to its spatial variation throughout all the calculations. This will therefore inhibit the radial (or the x-dependent) inhomogeneity in the system.

The configuration of Fig (3) is used as an initial condition for potential, which is then dynamically evolved using the set of governing Eqs. (1) & (2). The perturbed initial density is also initialized using the same condition, with a factor $(\epsilon_n - 1)/(\epsilon_n - u)$ before potential due to Eq. (4). The vorticity is constructed from potential, which is being updated at each time step using its value at previous times. Time sequence of evolution for a dipole vortex propagating along the y-direction is shown in Fig (4). It is clear from the figure that an exact nonlinear coherent solution of interchange mode turbulence in the form of a dipole vortex, travels in a straight line with a constant speed. The polarity of the dipole is such that left and right lobes of the dipole possess respectively negative and positive vorticity levels, while the net motion is along positive y-axis. Interestingly, when these polarities are altered, direction of the resultant motion is also reversed (not shown in the figure). The vorticity and the momentum associated with the translating dipole are conserved during the entire evolutionary process, and is shown in Fig (5). The dipole vortex here appears to be a long-lived and stable structure which survives for a period that is sufficiently longer than a few vortex-eddy turn over time i.e. $\tau_{\text{sim}} > \tau_{\text{eddy}}$, where $\tau_{\text{eddy}} = 2\pi/\Omega \simeq \pi$ as computed from simulations.

While the isolated dipolar vortex is stable during its translational motion, it is rather intriguing to see whether a direct collision of two oppositely propagating vortices is also stable. This is discussed in the subsequent section.

9

V. COLLISION OF TWO DIPOLES

We now consider collisional interactions of two dipole vortices. The vortices are propagating with equal and constant speed and heading towards each other in such a manner that they make a direct collision. Such study may, possibly, provide the most simplest understanding of turbulence phenomenon where presence of several coherent eddies can interact in a rather cumbersome manner thereby introducing various subtleties.

The initial configuration of two such dipole vortices placed at a certain distance apart from each other is shown in Fig (6-a). The polarities of their lobes have been chosen to make sure that they propagate in opposite direction with the same constant speed. In due course of time, the two vortices approach each other and eventually make a head-on collision as shown in Fig (6-b). Interestingly, during the time of collision and after it, the two vortices do not pass through each other, instead exchange their respective lobes. The positive lobe of dipole moving in $-y$ direction pairs with negative lobe of the dipole traversing along $+y$ direction and vice versa. The newly formed dipole vortices then continue to move in an orthogonal direction after the collision, as seen from the simulation in Fig (6-c,d). The overall trajectories of the colliding dipole vortices therefore exhibit a hyperbolic path, during which the total momentum before and after collision is conserved in the entire process. We also notice in all the simulations that the weak diamagnetic interaction (i.e. $\tau < 1$) has stabilizing effect on the interchange mode vortices.

When the two oppositely traveling dipole vortices are placed slightly off-axis and apart from each other initially, the collision interaction proceeds in a different manner than a pure head-on collision. The initial configuration is shown in Fig (7-a). In the off-axis collisional interaction, only co-rotating vortices interact with each other such that their translational speed is opposite. This is shown in Fig (7-b). Unlike pure head-on collision as discussed in Fig. 6, the two vortices in this case make their way past each other and continue to follow their initial path (as shown in Fig (7-c)). The resultant interaction however creates noticeable wake fields as seen in the figure where small scale contours of negligibly smaller magnitudes are clearly seen. The wake fields are also observed to be generated in the translational and head-on collisional studies, i.e Figs 4 & 6 respectively. Owing to a negligibly small magnitude of the wake field, they (wake field) do not appear to perturb or interact with the vortex flow field. Hence the propagating dipolar vortices remain intact amid the

wake field.

VI.   DISCUSSION

Nonlinear coherent structures are investigated within the paradigm of two dimensional electrostatic interchange mode turbulence. The model is often invoked to describe plasma phenomena associated with the curvature driven instabilities that occur near the tokamak edge region. It is shown that the self-organized coherent structures can exist in a turbulent system in the nonlinearly saturated state when all the linear instabilities are suppressed. This leads to an exact nonlinear stationary solution of the model equations amidst complex diamagnetic and polarization interactions. The coherent vortex essentially in the form of a dipolar configuration was shown to be an exact stationary and stable solution of interchange mode turbulence. The nonlinear studies based on translation, mutual interaction, and diamagnetic processes, show that the low frequency interchange mode dipole vortex is a long-lived and stable structure.

The dynamical properties of two dimensional interchange mode vortices investigated in isolation here could be useful in understanding more complicated processes such as collisional interaction amongst a large number of vortices, effect and interplay due to background interchange mode turbulence, effect of an inhomogeneous drift frequency and others. In the context of our analytic and simulation studies, one of the most important implications is that the coherent interchange vortices in the saturated edge turbulence can inhibit cross-field turbulent transport in the tokamaks owing to their robustness.

[1] A. M. Dimits, G. Bateman, M. A. Beer, et al. *Phys. Plasmas*, 7:969, 2000.

[2] B. N. Rogers, W. Dorland, and M. Kotschenreuther., Phys. Rev. Lett. **85**, 5336, (2000).

[3] M. N. Rosenbluth and F. L. Hinton., Phys. Rev. Lett. **80**, 724 (1998).

[4] G. W. Hammett et al., Plasma Phys. Controlled Fusion **35**, 973 (1993).

[5] M. A. Malkov, P. H. Diamond,and M. N. Rosenbluth Phys. Plasmas **8**, 5073 (2001).

[6] A. I. Smolyakov, P. H. Diamond, and M. Malkov., Phys. Rev. Lett. **84**, 491 (2000).

[7] Y. Hamada, T. Watari, A. Nishizawa, K. Narihara, Y. Kawasumi, T. Ido, M. Kojima, and K. Toi., Phys. Rev. Lett. **96**, 115003 (2006).

[8] N Miyato, Y Kishimoto1, and J Q Li, Plasma Phys. Control. Fusion 48 A335-A340 (2006)

[9] J. Zhao, T. Lan, J. Q. Dong, L. W. Yan, W. Y. Hong, C. X. Yu, A. D. Liu, J. Qian, J. Cheng, D. L. Yu, Q. W. Yang, X. T. Ding, Y. Liu, and C. H. Pan, Phys. Rev. Lett. **96**, 255004 (2006).

[10] Y Nagashima, K Itoh, S-I Itoh, K Hoshino, A Fujisawa, A Ejiri, Y Takase, M Yagi1, K Shinohara, K Uehara, Y Kusama and JFT-2M group, Plasma Phys. Control. Fusion **48** A377-A386 (2006).

[11] M. E. Austi et al., Phys. Plasmas **13**, 082502 (2006).

[12] Z. Lin, T. S. Hahm, W. W. Lee, W. M. Tang and R. B. White, *Science* **281** 1835 (1998).

[13] B. G. Hong and W. Horton, Phys. Fluids B **2**, 978 (1990).

[14] M. Ottaviani,F. Romanelli, R Benzi, M. Briscolini, P. Santangelo and S. Succi, Phys. Fluids B **2**, 67 (1990).

[15] J. Nycander, J. P. Lynov and J. J. Rasmussen, Europhys. Lett, 23 (4), pp.249-255 (1993).

[16] M. D. Tinkle and A. K. Sen, Phys. Plasma **3**, 4287, (1996).

[17] S. Dastgeer, R. Singh, H. Nordman, J. Weiland, A. Rogister, Phys. Rev. E., **66**, 036408 (2002).

[18] J. M. Finn, J. F. Drake, and P. N. Guzdar, Phys. Fluids, B **4** (9), 2758 (1992).

[19] W. Horton and A. Hasegawa, Chaos 4, 227 (1994).

[20] B. G. Hong, F. Romanelli, and M. Ottaviani, Phys. Fluids B 3, 615 (1991).

[21] V. D. Larichev and G. M. Reznik, Oceanology **16**, 547 (1976).

[22] J. D. Meiss, W. Horton, Phys. Fluids **4**, 990 (1983).

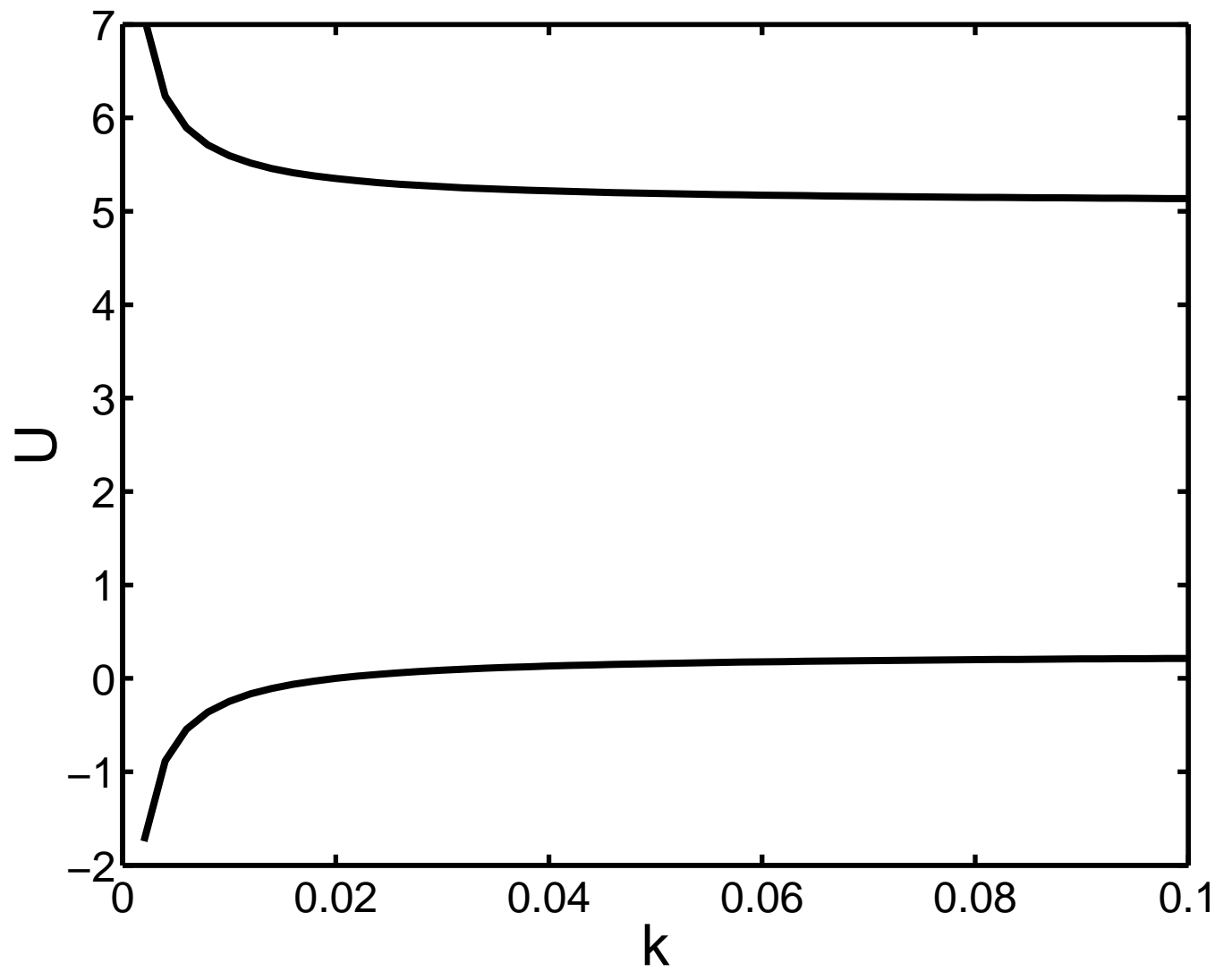[23] D. Gottlieb and S. A. Orszag, Numerical Analysis of Spectral Methods, SIAM, Philadelphia (1977)

FIG. 1: Allowed speed of coherent vortices. Upper branch corresponds to electron diamagnetic regime, while lower one represents ion diamagnetic regime.
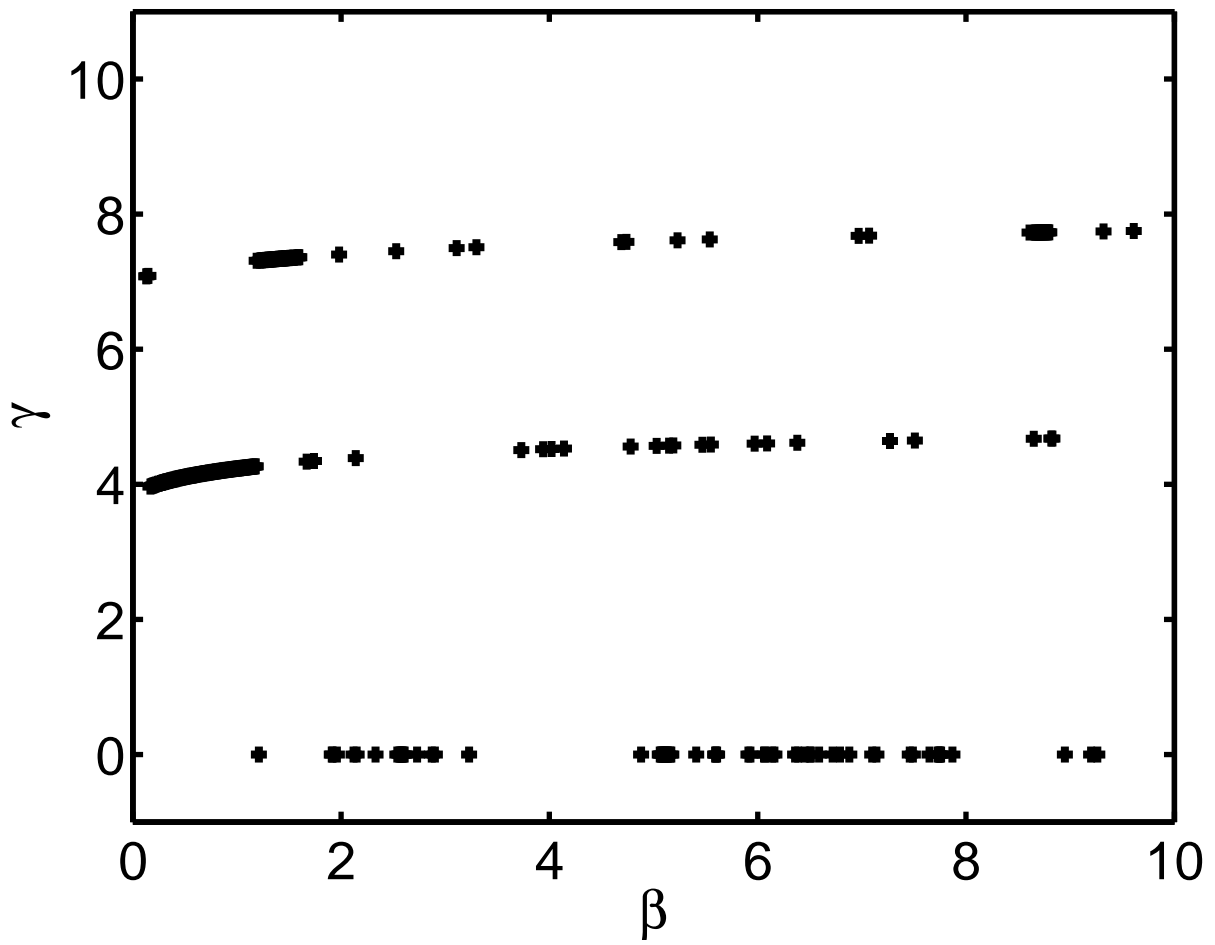
FIG. 2: Roots of nonlinear dispersion relation for typical parameters $a = 2.5, \tau = 0.1, u = 0.2, \epsilon_n = 0.4$. For a single value of β several branches of γ are borne out.
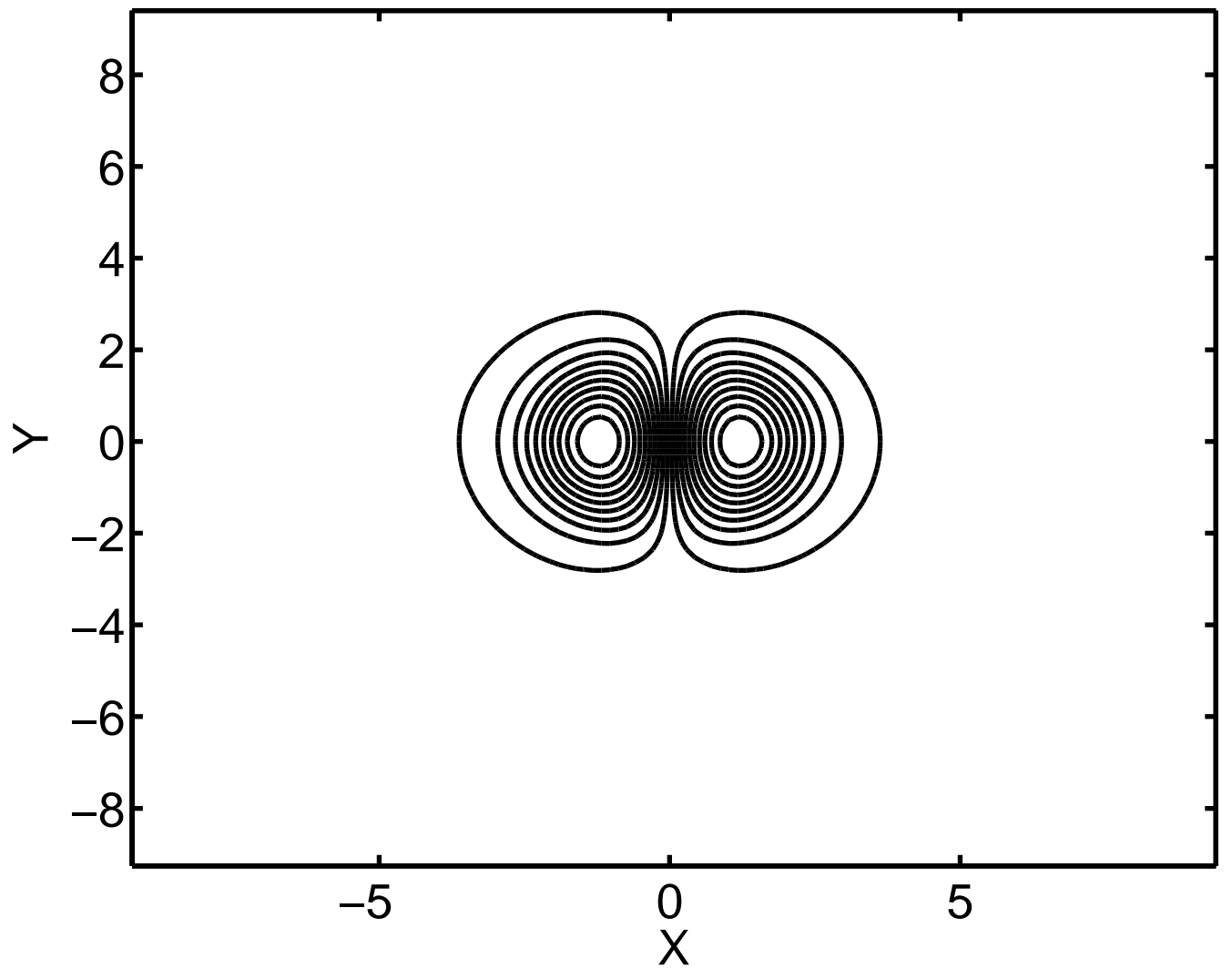
FIG. 3: Constant contour lines of the electrostatic potential in interchange mode turbulence. The spatial configuration is an analytically obtained dipole vortex solution with radius $r = 2.5, \beta = 5.9, \gamma = 1.3$ while other parameters are $\epsilon_n = 0.4, \tau = 0.1$.
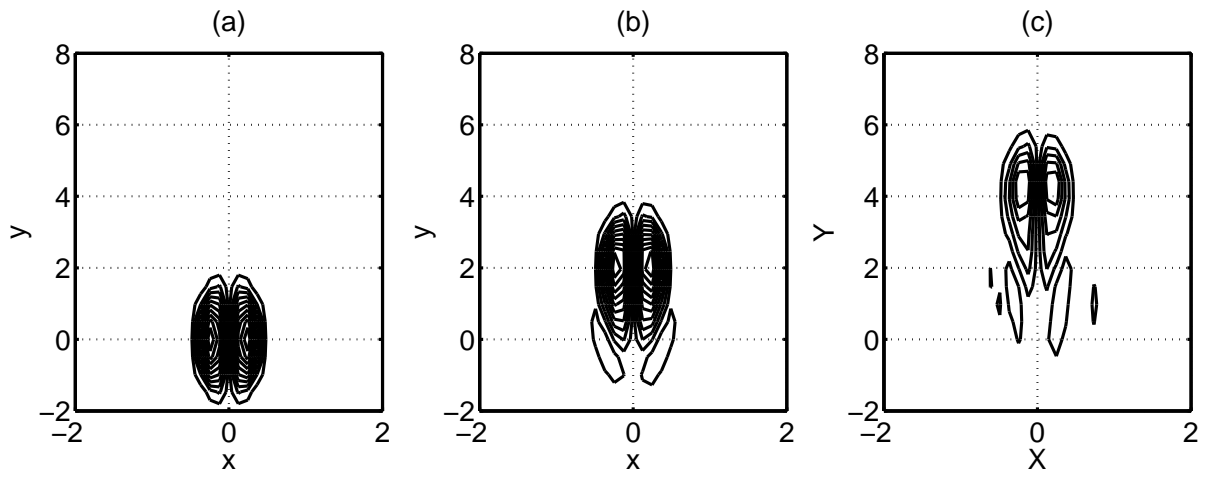
FIG. 4: Simulation results of a propagating dipole vortex in interchange mode turbulence at three different time $t = 0, 7, 15$ corresponding to (a), (b) and (c). The sign of the vorticity level for left and right lobes of the dipoles are respectively negative and positive. The resultant motion is along the positive y-direction. When the polarities are reversed, the direction of propagation is also reversed (not shown here).
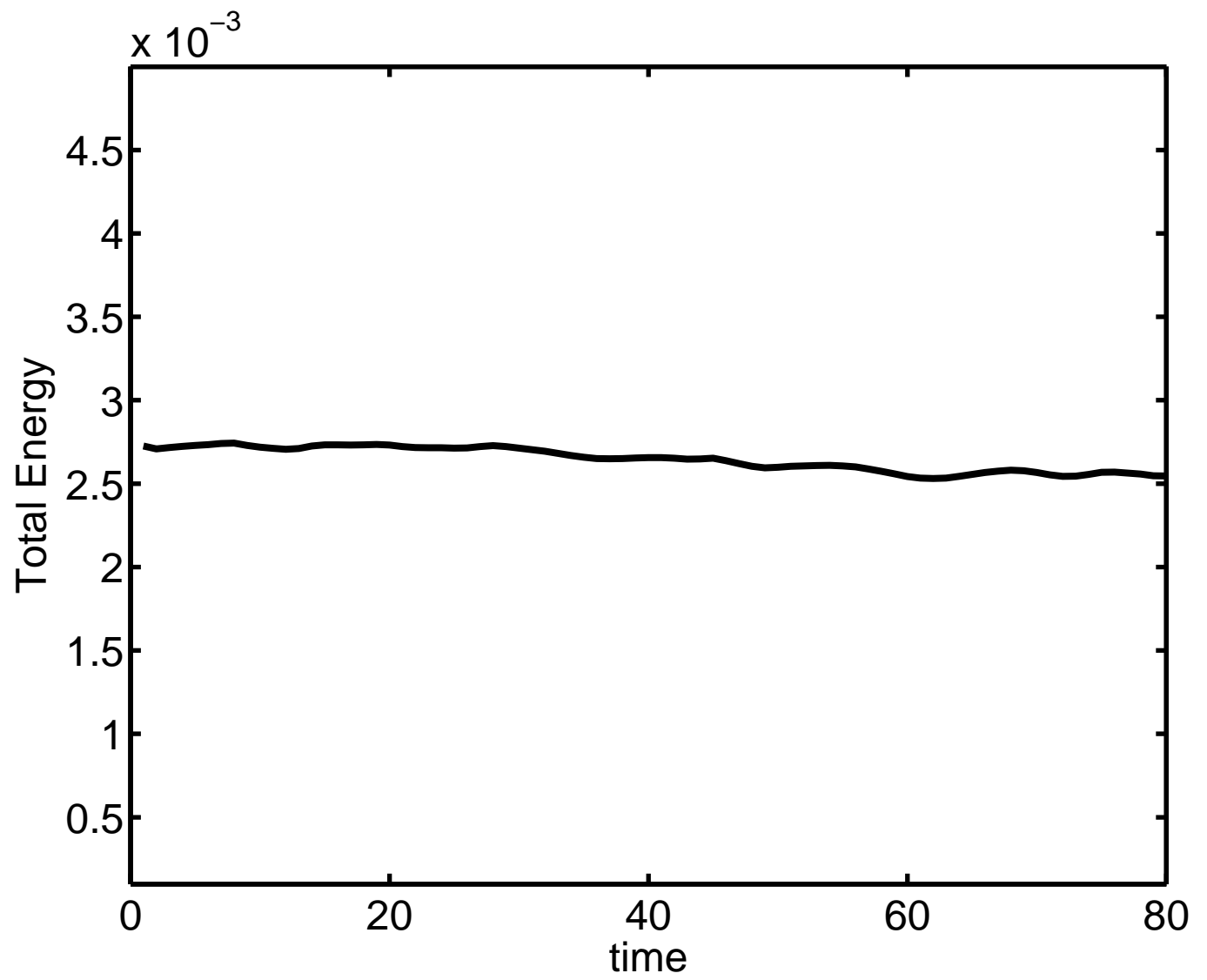
FIG. 5: Conservation of vorticity in the simulation when the damping terms are zero ($\mu = D = 0$).
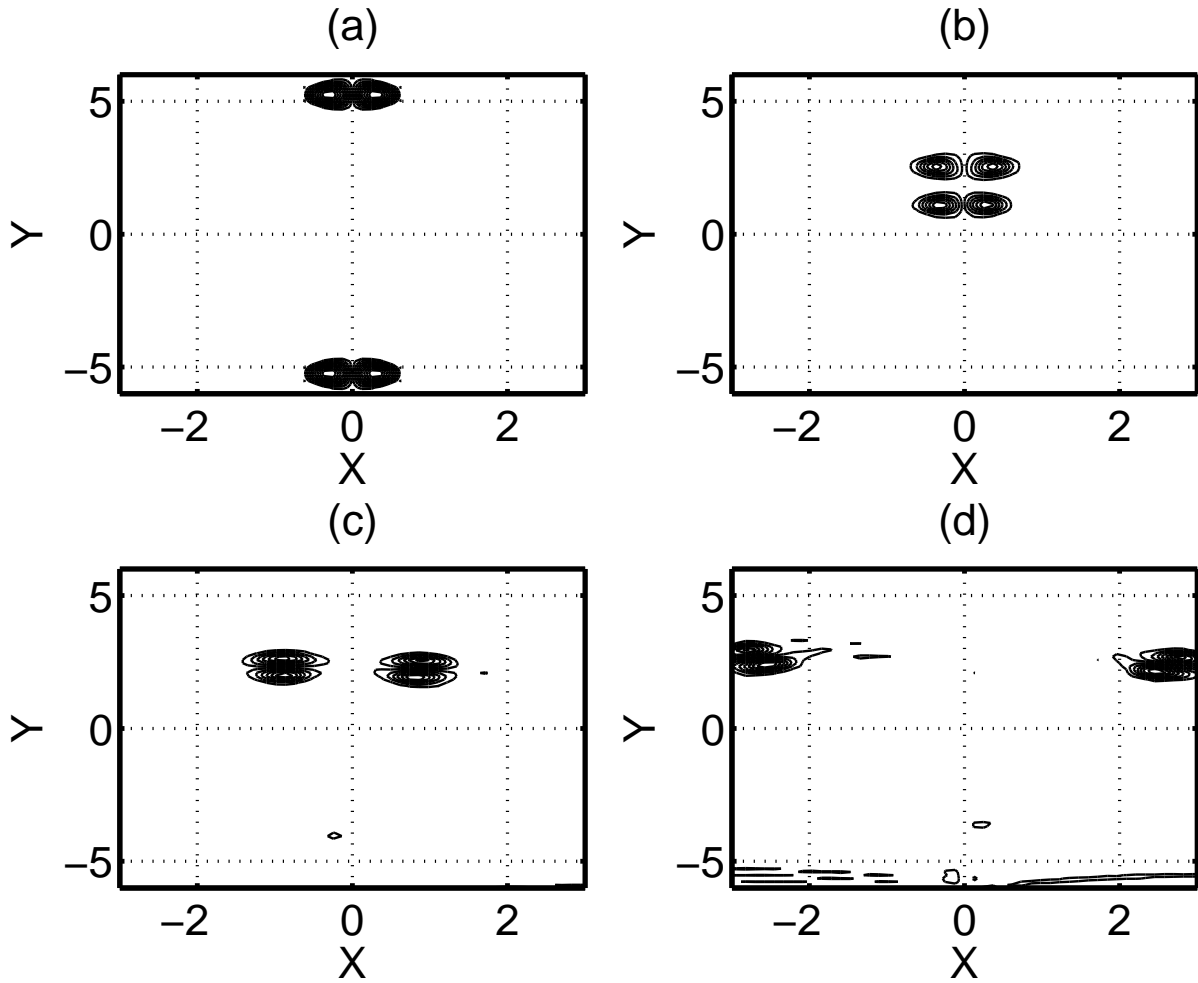
FIG. 6: Head-on collision of two dipole vortices in interchange mode turbulence. The vortices are traveling in the opposite direction with the constant speed [see (a)], and eventually make a collision as seen in (b). The collision appears to be perfectly elastic. An exchange of pair of their vorticities lobes occurs [see (c)]. The newly formed dipole vortices then continue to move in orthogonal path [see (d)]. The overall trajectory, before and after collision, thus appears to be hyperbolic.
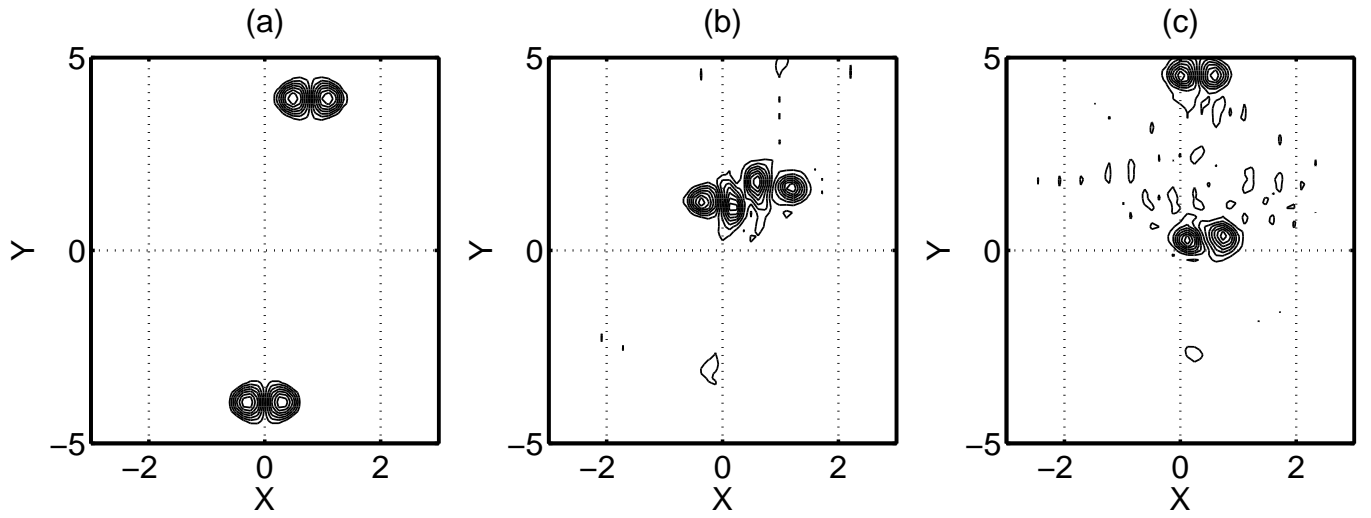
FIG. 7: Off-axis head-on collision of two oppositely traveling dipole vortices in interchange mode turbulence. During collisional interaction, only co-rotating vortices interact with each other such that their translational speed is opposite. Unlike pure head-on collision as discussed in Fig. (6), the two vortices in this case make their way past each other. The resultant interaction however creates noticeable wake fields as seen in the figure (small scale contours of negligibly smaller magnitudes).